Journal of Power Sources, 43–44 (1993) 317–326

A high power lithium thionyl chloride battery for space applications

Pinakin M. Shah
Alliant Techsystems Inc., Power Sources Center, 104 Rock Road, Horsham, PA 19044 (USA)

Abstract

A high power, 28 V, 330 A h, active lithium thionyl chloride battery has been developed for use as main and payload power sources on an expendable launch vehicle. Nine prismatic cells, along with the required electrical components and a built-in heater system, are efficiently packaged resulting in significant weight savings (>40%) over presently used silver–zinc batteries. The high rate capability is achieved by designing the cells with a large electrochemical surface area and impregnating an electrocatalyst, polymeric phthalocyanine, $(CoPC)_n$, into the carbon cathodes. Passivation effects are reduced with the addition of sulfur dioxide into the thionyl chloride electrolyte solution. The results of conducting a detailed thermal analysis are utilized to establish the heater design parameters and the thermal insulation requirements of the battery. An analysis of cell internal pressure and vent characteristics clearly illustrates the margins of safety under different operating conditions. Performance of fresh cells is discussed using polarization scan and discharge data at different rates and temperatures. Self-discharge rate is estimated based upon test results on cells after storage. Finally, the results of testing a complete prototype battery are described in detail.

Introduction

Silver–zinc primary active batteries are presently in use to power most expendable launch vehicles. In addition to being very heavy, this electrochemical system imposes many operating restrictions like limited time window for launches, specific thermal insulation requirements based on expected environment, etc. The lithium thionyl chloride battery being developed would save over 40% of the battery weight and considerably relax the restrictions to result in significant cost savings.

Alliant Techsystems Inc. has designed and developed a lithium thionyl chloride battery as a 'drop-in' replacement for the silver–zinc battery currently used on a launch vehicle. A minimum capacity of 250 A h is required for the mission after six years of controlled storage (at −18 °C) and up to one year of uncontrolled storage at temperatures between 4.4 and 32.2 °C. The unique design of this battery, its analyses, and performance are described in this paper.

Battery design

The battery consists of nine prismatic cells connected in series and efficiently packaged in an aluminum housing with a built-in heater system. The housing is an

0378-7753/93/$6.00

Fig. 1. A high power lithium thionyl chloride battery for space applications.

integral box with no welds or joints and is fabricated by conventional and electrical discharge machining processes. It contains ten cavities, nine to house individual cells and the tenth to package electrical circuits, thermostats, and external connectors. Figure 1 shows the photograph of a typical battery. Each cell is rigidly bonded to the cavity walls by means of an epoxy. The cells are connected to each other and to the external connectors by means of solid copper busbars which are silver plated where exposed to the environment. All electrical paths and connections outside the cells are designed such that their total resistance does not exceed 4.5 mΩ. A fully redundant, single fault tolerant, foil heater has been integrally designed into this battery to provide uniform heating to each cell when the thermostats sense the battery temperature falling below the set point. A temperature transducer is also located at the center of the battery in the long web to monitor the maximum battery temperature through one of the external connectors. A translucent, remove before flight, snap-on, plastic cover has been designed to fit the top of the battery.

The overall battery dimensions are 337 mm (L)×231 mm (W)×257 mm (H) which are significantly smaller than those for the silver–zinc battery. However, the mounting feet are designed to match the footprint of the latter. The typical weight of this battery is 35.4 kg.

Cell design

The cell design is prismatic with two terminals (case neutral), balanced lithium and carbon capacities, and excess electrolyte. A large number of anode and cathode assemblies are stacked up alternately with glass separators between them. The current collectors for both electrodes are chemically etched from 0.15 mm thick nickel foil and have leads as their integral parts. The electrode stack is inserted into the cell case and held tight inside by means of supports in all axes. The leads are bent and brought together at their respective glass-to-metal seal terminal blades and bolted. Welds are additionally made to provide redundant electrical contact and protection

from bolt loosening during vibration. The case is 316 L stainless steel, thin walled, and capable of withstanding stringent shock, vibration, and thermal environments only when cells are packaged in the battery structure. The header plate is structurally self-supporting and contains a safety pressure vent in addition to the two glass seals. The overall cell dimensions are 107 mm (L)×56 mm (W)×224 mm (H), not measuring the terminals and it weighs an average of 2.9 kg.

In addition to the large electrochemical surface area provided (9686 cm^2), an electrocatalyst, polymeric cobalt phthalocyanine $(CoPC)_n$, is impregnated into the carbon cathode matrix to achieve high rate capability. The performance and stability of this catalyst in active lithium thionyl chloride system has been demonstrated earlier [1]. Sulfur dioxide is added to the electrolyte solution to improve cells' initial voltage delay behavior after active storage presumably via changes in morphology of the passivating film [2]. The design with regard to electrochemical parameters like stack compression, carbon cathode thickness, current density, etc., was guided by the results of extensive studies conducted earlier [3]. The cell has a nominal fresh capacity of 330 A h which is sufficient to guarantee a minimum of 250 A h for the mission after providing for storage losses and cold temperature derating.

Thermal analysis

The batteries are mounted on the outside of the vehicle's forward adaptor which exposes them to an uncontrolled thermal environment in space. A detailed thermal analysis is therefore necessary to ensure proper design and operation of the batteries. A two-phase approach was selected. The battery was considered to be a point mass (single node) in the first phase to expeditiously carry out parametric analysis. In the second phase, a detailed, multinodal, finite element model (FEM) was constructed using ANSYS program on a VAX computer. Specific boundary conditions were imposed to establish temperature–time profiles for each of the nodes.

The specification [4] defines parameters that help calculate various heat fluxes in space for two extreme conditions — worst case hot (WCH) and worst case cold (WCC). Heat balance equations on the battery are established by equating the heat generation and heat loss terms. For WCC, the only heat generation term is due to the battery discharge whereas losses occur due to radiation to space and vehicle and conduction through mounting feet. For WCH, the heat absorbed by the battery also includes free-molecular heating and radiation from the sun and the earth. Conduction losses through mounting feet are ignored. Heat generated by the discharge process was calculated using an effective thermoneutral potential, ETNP, of 3.85 V.

Solving the heat balance equations for single node thermal analysis provides the average battery temperature profile for the duration of the mission. Typical results for a couple of WCH conditions are presented in Fig. 2. The results for various conditions of interest are summarized in Table 1. These clearly illustrate that, if the thermal environment for a mission can be predicted, appropriate amount of insulation can be applied for optimum battery operation. However, if the environment is not predictable, a fixed level of insulation cannot ensure safe and proper battery operation under both WCC and WCH conditions. It is therefore imperative that a battery with no insulation be selected and in-flight heaters be provided to maintain the minimum operating temperature for adequate performance under WCC conditions.

Minimum operating temperature of 15 °C was selected based upon the electrochemical performance data (see later). Maximum heater power required is calculated

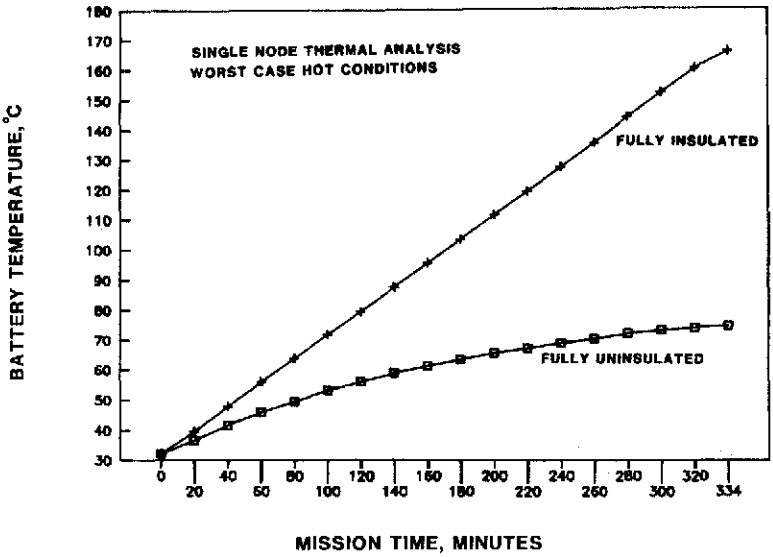

Fig. 2. Projected battery temperature profile.

TABLE 1

Summary of single node thermal analysis results

Case	Percent adiabatic coverage (insulation)			Temperature at mission end (°C)	
	Top	Bottom	Sides	WCH (32.2 °C)	WCC (4.4 °C)
1	0	0	0	+74.6	−40.7
2	0	0	100	+115.9	+7.0
3	0	100	100	+128.4	+28.1
4	100	100	100	+165.8	+72.9

by fixing the average battery temperature to 15 °C in the single node heat balance equation for WCC. The actual heater elements' capacity is sized according to Mil-Std-1540B specification. Sensitivity studies showed that the ETNP value has a significant impact on the results with a lower value reducing the maximum battery temperature under WCH conditions and increasing heater power/energy consumption under WCC conditions.

Multinodal FEM thermal analysis was carried out for WCH conditions to ensure the battery will operate safely without venting. Furthermore, the hottest point in the battery was identified to locate the temperature transducer in its vicinity. Similar analysis for WCC conditions was performed to determine the coldest spot on the battery. The thermostats controlling the heater function were located there. Heater elements cycling rate was also determined to be acceptable for WCC conditions.

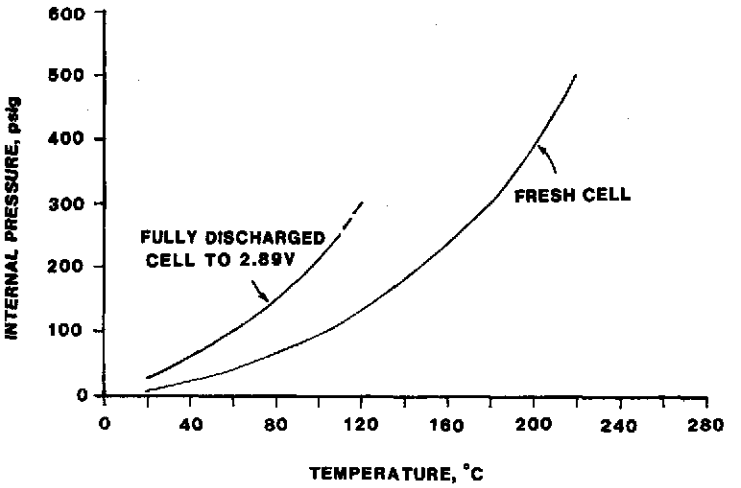

Fig. 3. Internal cell pressure vs. temperature.

Structural design considerations

In addition to the extremes of thermal environments that the battery is designed for, it must also be capable of withstanding severe shock and vibration conditions encountered during launch and payload separation. The vibration specification calls for a random input of 13.7 g RMS in the frequency range of 20 to 2000 Hz with a peak g^2/Hz of 0.5. This specification is applied for 180 s in each of the three axes. The shock spectrum spans from 100 to 3000 Hz with peak acceleration ranging from 80 to 2000 g in both positive and negative directions. Three such shocks are applied successively in each of the three axes. These parameters define the dynamic loads that the battery structure is subjected to.

Statically, the specification requires the battery to not yield up to the vent operating pressure and to not fail at twice that pressure. The maximum operating pressure (MOP) for cells was selected to be 200 psig (1.38 MPa) which will be experienced in a fully discharged cell at 100 °C (Fig. 3). The safety vent is designed to operate at 300 psig (2.07 MPa) at 150 °C. The battery structure has been designed, with sufficient margins, to not yield at 325 psig (2.24 MPa) and to not fail at 650 psig (4.48 MPa).

The battery housing takes advantage of a ribbed structure to support the static loads on two broad faces of the cells. The number, thickness, spacing, and manufacturability of the ribs were optimized to minimize weight. The other two walls are designed with curved walls in each cell cavity similar to the concept utilized in large inflated domes. The battery housing is machined starting from a solid rolled plate or a forged block of aluminum. No welds of joints are present to achieve maximum strength for the weight. The mounting gussets and handling features are also integral parts of this housing. This unique approach has limited the typical weight of this housing to 6.1 kg.

Internal pressure/vent design analysis

The cells are designed to operate safely under normal use. In other words, the vent will not burst open under normal conditions; however, it will operate well before

the melting point of lithium is approached in an abusive condition leading to thermal runaway.

Figure 3 shows the vapor pressure curves for a fresh and a fully discharged cell. Since the composition of the discharged electrolyte is not precisely known, actual cells in discharged conditions were employed to generate these data. It should be noted that the vapor pressure at the end of the mission will be lower because that condition equates to only 250 A h of discharge capacity whereas the cells used to generate the data in Fig. 3 delivered > 300 A h.

As the discharge progresses, internal changes take place in the cell according to the following reaction:

$$4Li_{(s)} + 2SOCl_{(l)} \longrightarrow 4LiCl_{(s)} + S_{(s)} + SO_{2(l)} \quad (1)$$

During discharge, there is a net 28% reduction in the volume of active materials thereby increasing the void volume in the cell. However, temperature rise associated with discharge slightly reduces this effect.

Figure 4 graphically presents a comprehensive analysis of the cell's safety under different conditions. The solid lines represent the nominal conditions and the dashed

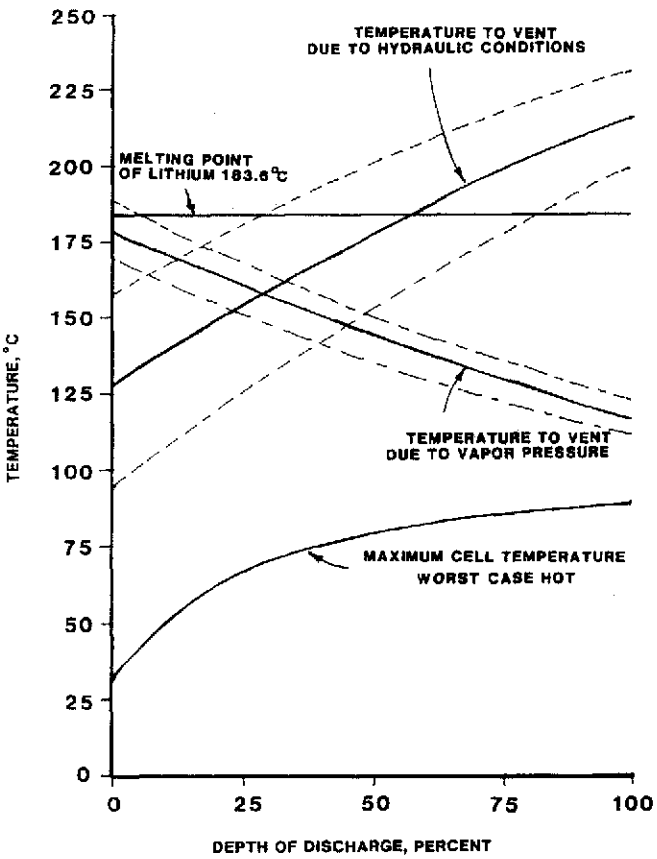

Fig. 4. Internal pressure/vent design analysis.

lines show the upper and lower limits of theoretical tolerances which, for all practical purposes, have zero probability of occurrences. Clearly, for discharge states below the point where the two 'temperature to vent' lines intersect, the cells would vent due to a hydraulic condition if the temperature rose for any reason. Above that point, the cell internal pressure will exceed the vent burst pressure prior to reaching a hydraulic condition. In either case, the cells would vent well before the melting point of lithium is reached. The graph indicates that sufficient margin of safety exists even under the highly improbable extreme conditions of tolerances. Similarly, the operating vent temperature line is well above the maximum cell temperature profile predicted by thermal analysis for worst case hot conditions.

Performance characteristis

Figure 5 shows typical discharge profiles for fresh cells at a continuous 42 A rate with pulses at 60 and 75 A. Two thick aluminum plates were utilized to maintain the broad faces of the cell flat during discharge testing. The test set-up permitted only natural convection and radiation from the cell walls to simulate battery conditions in space. The starting cell temperatures were stabilized at 4.4 and 23.8 °C. The operating voltages are well above the minimum requirements and capacities of approximately 360 A h are realized.

Fresh cell discharge voltage characteristics are presented in Fig. 6 at different temperatures and two depths-of-discharges (DOD). The first DOD level chosen (3.2%) represents initial behavior of cells after passivation effects are overcome and the second level (75%) represents the point where a 60 A 30 min pulse begins and the internal resistance of the cells starts to gradually rise. It is evident from these data that the minimum set point for the thermostats controlling the heater function should be 15 °C in order to achieve at least 3.25 V. The high operating voltages observed especially at high load currents are attributed to the presence of the catalyst in carbon cathodes.

The discharge characteristics of cells after storage are significantly influenced particularly in the initial stages by the passivation phenomenon. This was discussed in detail earlier and preconditioning methods were established to restore cells' behavior to prestorage conditions [1]. Figure 7 compares the discharge profiles of cells fresh and after three months of storage at 32.2 °C. Although capacity is reduced by 8.3%,

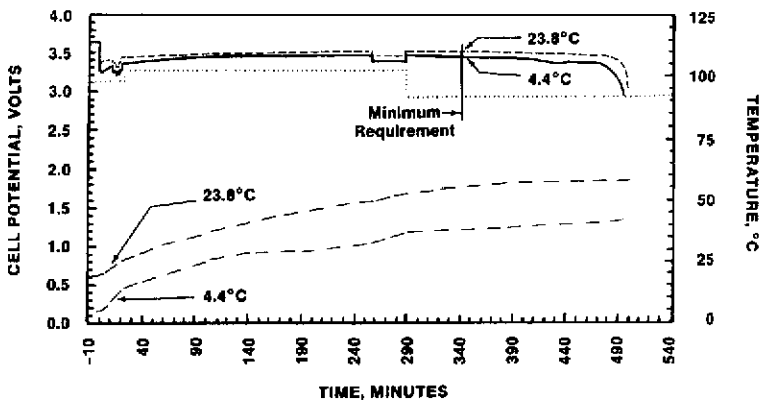

Fig. 5. Fresh cell discharge performance.

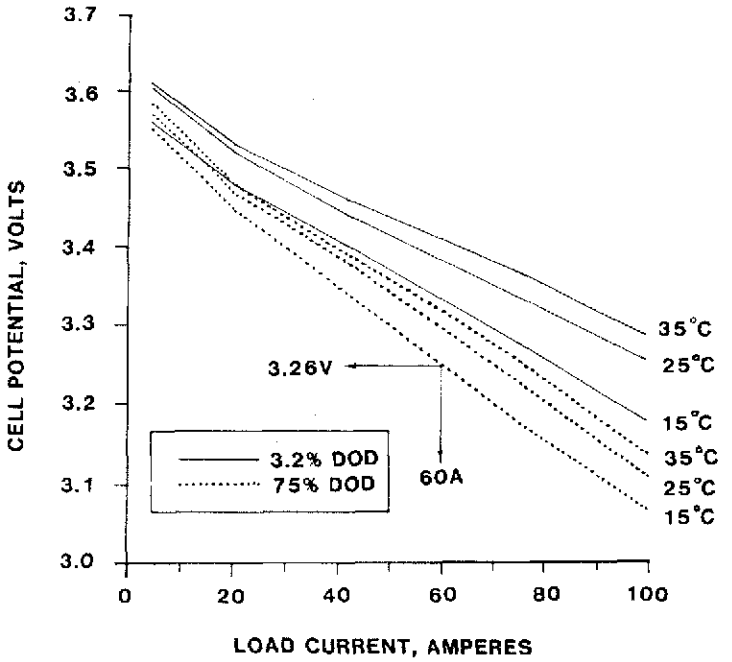

Fig. 6. Cell voltage characteristics.

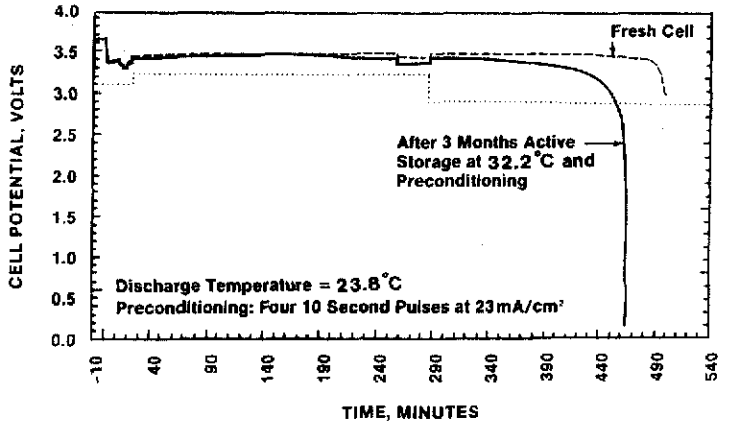

Fig. 7. Cell discharge performance after storage.

the voltage level is comparable with that of a fresh cell. Similarly, Fig. 8 presents voltage profiles of cells after storage for six months at 23.8 and 32.2 °C followed by preconditioning. The temperature of storage apparently has a noticeable effect on the initial voltage levels presumably because higher temperature forms a film tougher to clean. The capacity loss was 11.7%; however, preconditioning was not completely effective in cells stored at 32.2 °C for six months. Similar effect was noted in other cells stored for one year at 32.2 °C. The preconditioning was even less effective and

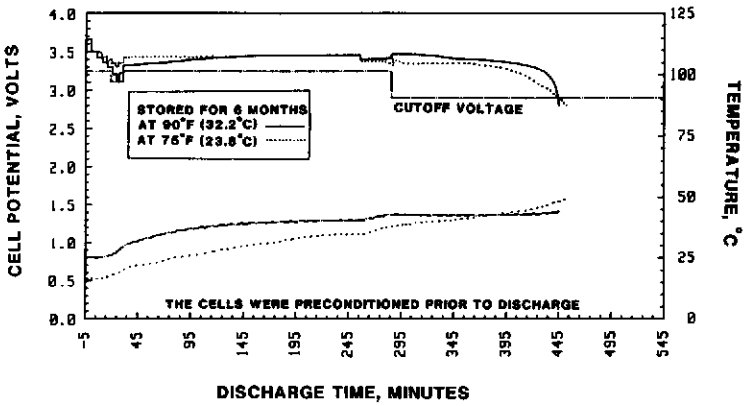

Fig. 8. Cell discharge performance after storage.

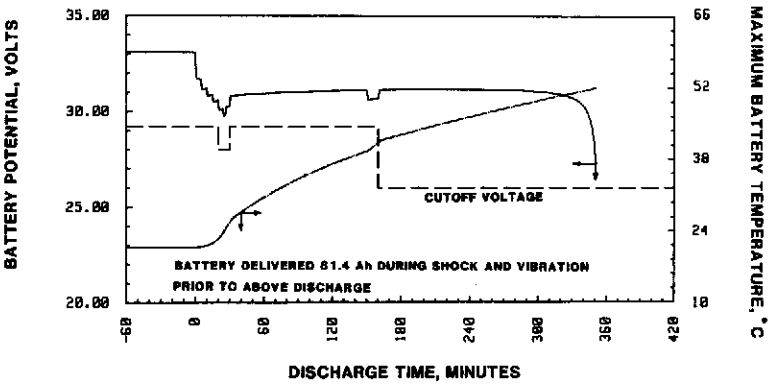

Fig. 9. Battery high rate discharge performance.

the voltage delay was severe resulting in voltages below the minimum requirement for over 60 min of discharge. The selected method for preconditioning seemed to be effective for storage up to six months at 32.2 °C and up to one year at 23.8 °C. Beyond that, a more aggressive method is required.

A prototype battery was assembled to demonstrate its ability to meet the requirements of the application. It was instrumented to monitor not only the battery voltage and temperature but also individual cell voltages and temperatures at the top of each cell. Vibration tests were conducted while the battery was under 42 A continuous load and all parameters were recorded before, during, and after the test. No abnormalities in cell/battery behavior were noted during 180 s of random vibration in each of the three axes. The battery was then subjected to shock tests, again while under a continuous 60 A load. Three shocks in each of the three axes produced no abrupt changes in voltages or temperatures. Capacity delivered by this battery during shock and vibration tests was 81.4 A h. The battery was then discharged under ambient conditions at the high rate profile. Figures 9 and 10 show the results of this discharge test. Clearly, the battery delivered voltages well above the minimum requirement and the individual cells were very consistent. All the cells were at the knee of their discharge curves at the completion of the test. The total capacity delivered by this battery was

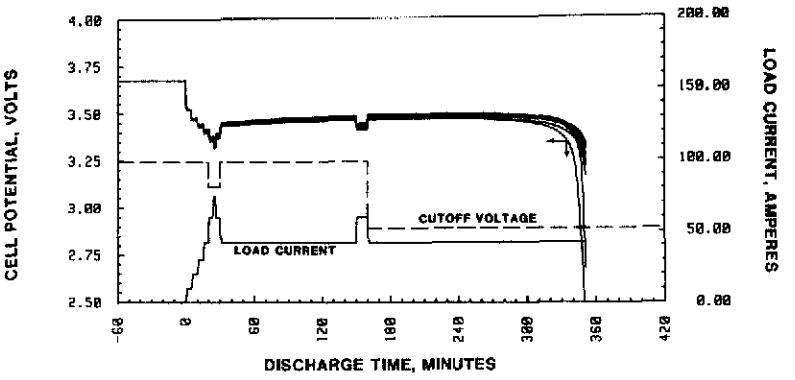

Fig. 10. Individual cell voltage profiles during battery high rate discharge.

327.7 A h and the peak temperature reached was 54 °C. Destructive physical analysis of this battery and all nine cells after completion of these tests revealed all the components to be in their normal expected condition. No evidence of any damage due to shock and vibration was noted.

Conclusions

Alliant Techsystems Inc. has developed an active, high rate, lithium thionyl chloride battery capable of meeting the stringent requirements for space applications. The unique approach to battery housing design and cell packaging has resulted in a safe, rugged, and lightweight power source. The technology developed will undoubtedly find many uses because of the ease with which the product can be scaled up or down. The various analyses and tests conducted in this program support the claim that sufficient margins exist in all aspects of this battery design.

Acknowledgements

The author wishes to acknowledge contributions made by Robert J. Horning, William J. Eppley, Stan N. Schwantes, Charles J. Kelly, John H. Kim, William F. Brown and other support staff at Alliant Techsystems Inc.

This work was performed for the Jet Propulsion Laboratory, California Institute of Technology. Reference herein to any specific commercial product, process, or service by trade name, trademark, manufacturer, or otherwise, does not constitute or imply its endorsement by the United States Government, Alliant Techsystems Inc., or the Jet Propulsion Laboratory.

References

1 P. M. Shah, *Proc. 34th Int. Power Sources Symp., Cherry Hill, NJ, USA, June 25–28, 1990,* p. 222.

2 D. L. Chua and W. C. Merz, *US Patent No. 4 309 490* (1982).

3 N. Doddapaneni and N. A. Godshall, *Proc. Symp. Primary and Secondary Ambient Temperature Lithium Batteries, Honolulu, HI, USA, Oct. 18–23, 1988,* Proc. Vol. 88-6, p. 175.

4 *General Dynamics Specification, No 57-06000 Revision A,* Mar. 15, 1990.